Development of a 2.5D Representative Volume Element model of AlSi10Mg material produced by additive manufacturing

C. Bouffioux, L. Papeleux, S. Tran,
J-P. Ponthot, L. Duchêne, A. M. Habraken

LIÈGE université
Urban & Environmental Engineering

27-04-2022 ESAFORM 2022 Braga PT

Content

- Target application and methodology
- Features of AlSi10Mg FSP microstructure
- Nanoindentations
- RVE development and validation
- Conclusions

Long Life AM project - Experimental context

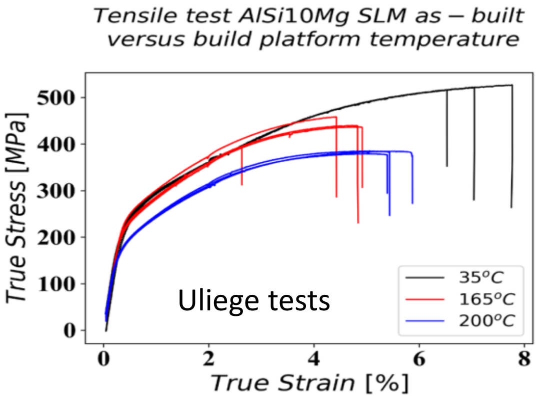

As built microstructure AB (Cells)
(Santos Macías et al., Acta Materialia 201, 2020)

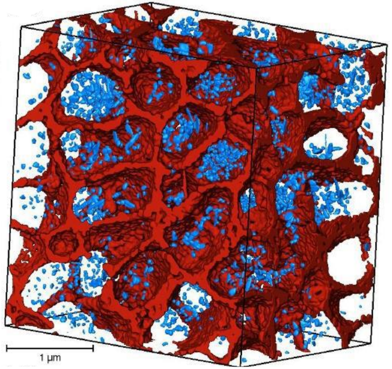

Post treatment effects (thermal treatment TT1, TT2 or Friction Stir Processing FSP)

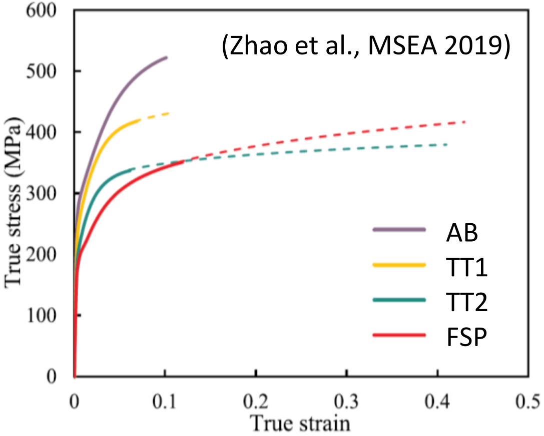

+ DSC, SEM, DRX
→ Microstructure
Evolution AB

Nano indentation
→ **Local mechanical properties**

FSP ↑ ↑ **Fatigue life**

Cells

Matrix + Precipitates

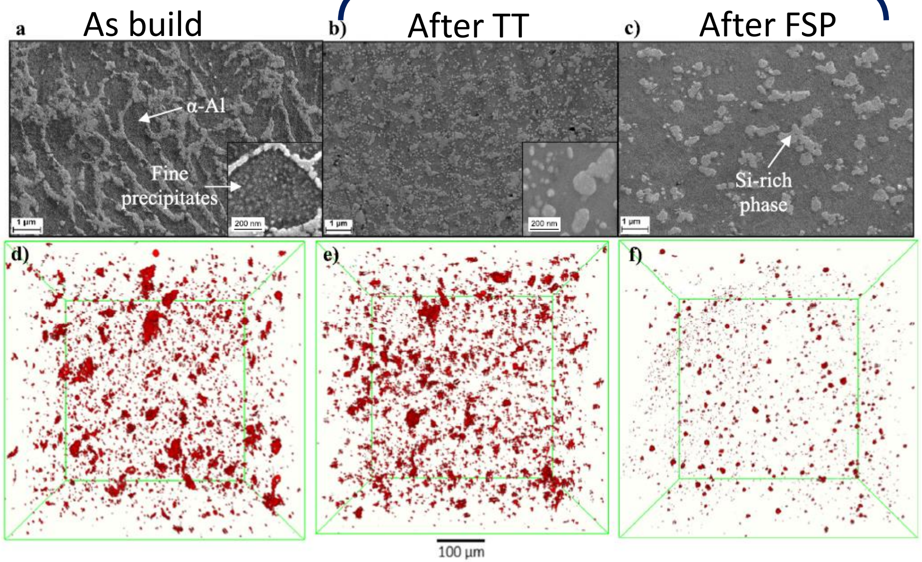

(Santos Macías et al., Scripta Materialia 170, 2019)

Towards Numerical Material Design

Microstructure Design through RVE

OM, SEM or results of PF
⇩
Microstructure EF meshes

\+

Representative Volume Element RVE

\+

Nanoindentation for local material properties

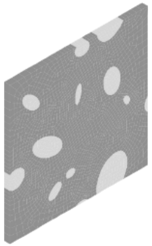

AB & internal TT (35°c 165°c 200°C)
AB & TT post treatment
AB & FSP post treatment
AB 1st runt DSC
AB 2nd run DSC

→

σ - ε curve
Damage mechanism
Static
Fatigue

Applied tensile strain

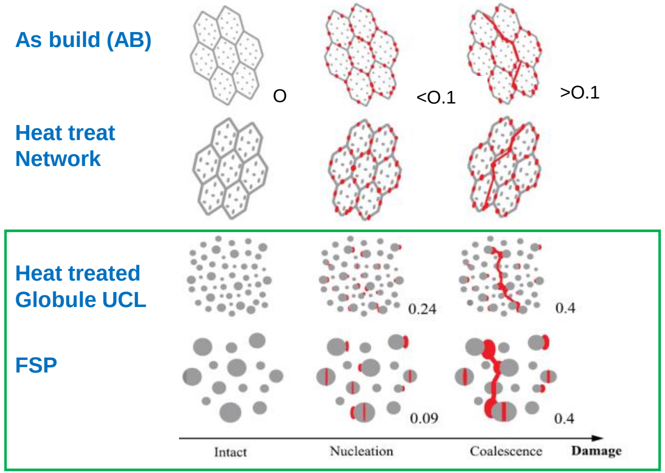

(Zhao et al., MSEA 2019)

Statistical observations taken into account to build RVE

(Zhao et al., MSEA 2019)

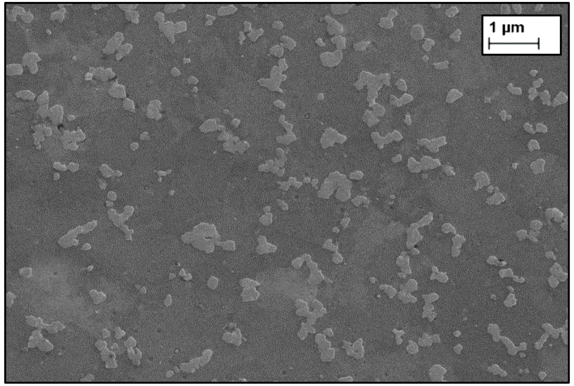

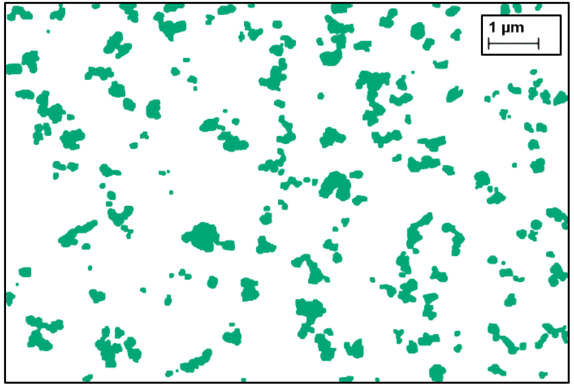

Post treatment ULiege

Si particles described by equivalent ellipses:

- equivalent circle diameter $\varnothing_{eq}$ [0.118; 0.695] µm
- aspect ratio: AR = $\varnothing_{min}$ / $\varnothing_{max}$
- angle major axis / horizontal axis of image: α
- Pearson correlation coefficients: r

→ higher rate of small particles

→ few elongated grains

→ no dominant orientation angle

→ weak correlations between $\varnothing_{eq}$, AR, α

Nanoindentations: grid α-Al or single target indent Si

case of matrix + particle material

Si particle:

Elastic behavior characterized from literature & Si nanoindentation

(Dedry et al., ESAFORM PoPuPs, 2021)

α-Al matrix elasto-plastic behavior:

- Inverse modelling (Berkovich indenter, based on the total set of available curves)

  Tran H.S. et al. 2022 (revision Int. J. of Mech. Sc.)

- Dao & Bucaille method (3 ≠ indenters, use of lower curves of the grid)

  Bouffioux C. et al. (soon)

α-Al matrix characterization by Berkovich & inverse modelling

Finite Element Inverse model of lowest curve: assumed α-Al → data set A

Sensitivity analysis of indent position and size of Si

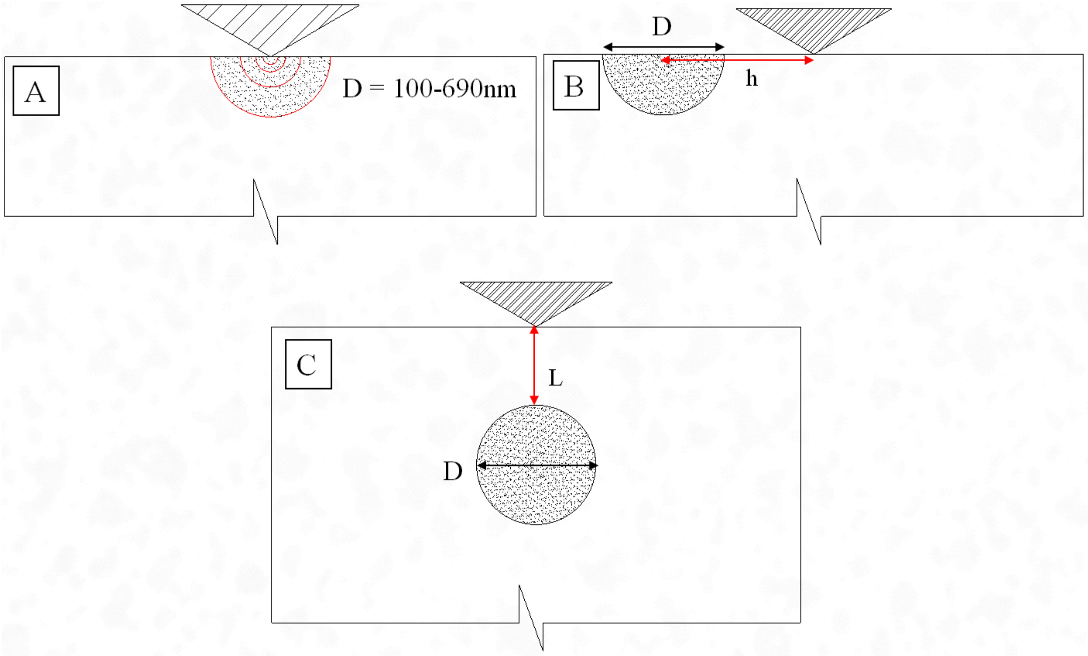

Berkovich

$\sigma_{y,\ \alpha\text{-Al}} / \sigma_{y,\ Si} = 0.036$

D [0.118; 0.695] μm

Si of D < 0.2 μm

→ not effect on force-displacement curve

Indent further than 0.345 μm from Si particle

→ α-Al matrix behavior

α-Al matrix characterization by Berkovich & inverse modelling

Data set A validation

Range of simulations and experiments

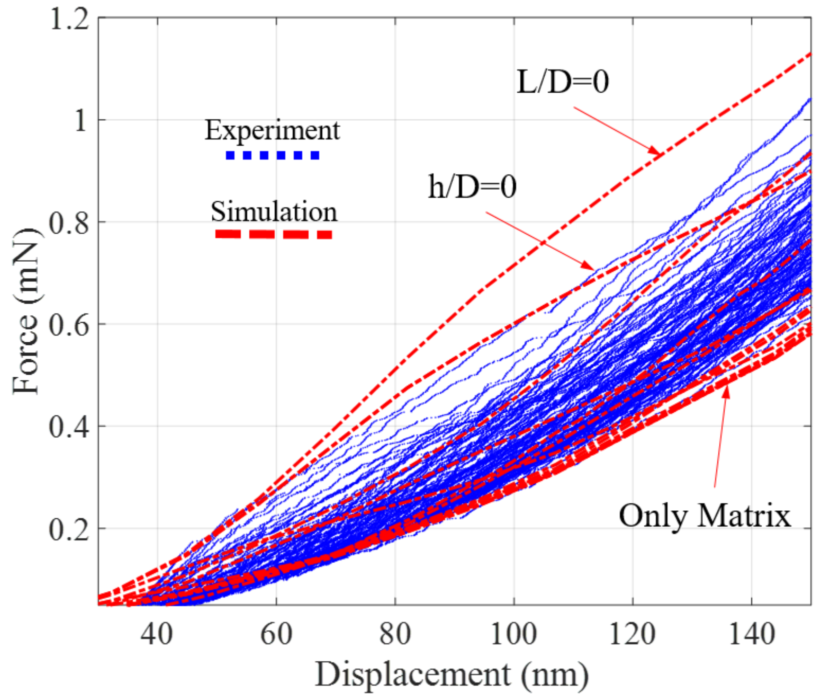

Prediction / Experiment of cube corner

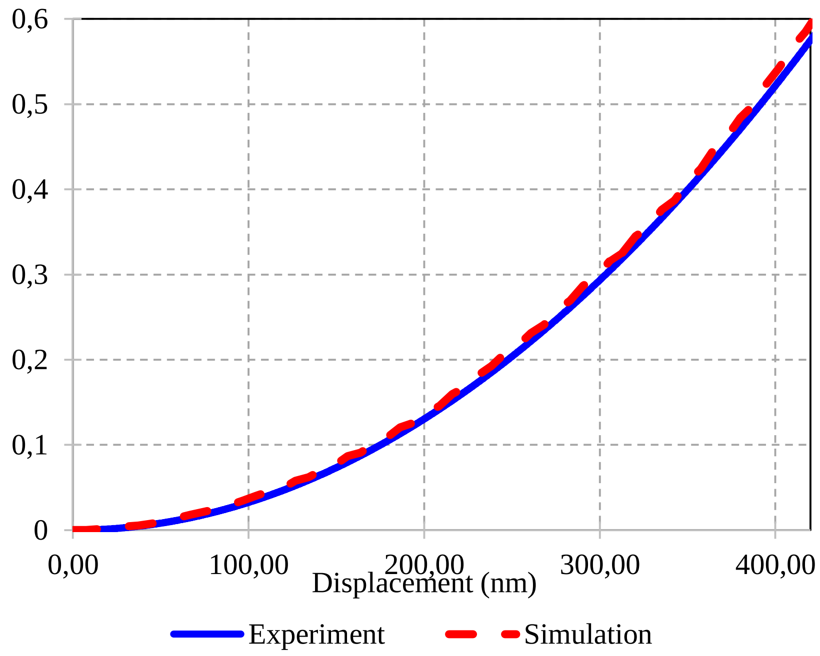

α-Al matrix characterization by nanoindentations & Dao-Bucaille

1 point ($\varepsilon_{r,\theta}$, $\sigma_{r,\theta}$) for each indenter characterized by its angle α

- **Nanoindentation curves**

→ $F = C_\theta . h^2$ with F: normal force, h: penetration depth, C_θ: constant

→ $$\frac{1}{E^*} = \frac{1-\nu^2}{E} + \frac{1-{\nu_i}^2}{E_i}$$ with E*: reduced modulus of the curve

- **K.L. Johnson (J. Mech. Phys. Solids, 1970)** → characteristic strain $\varepsilon_{r,\theta}$ per indenter

→ $\varepsilon_{r,\theta} = K . cotan(\theta)$ with θ: angle of the equivalent cone, K = 0,105 (Bucaille, Acta Mat. 51, 2003)

→ $$\theta = arctan\left(\sqrt{\frac{3.\sqrt{3}}{\pi}}.tan(\alpha)\right)$$ with α: angle of indenter

- **Dao's method (Acta Mat. 49, 2001) + Bucaille method (Acta Mat. 51, 2003)**

→ $$\Pi_{1\theta} = \frac{C_\theta}{\sigma_{r\theta}} = tan^2(\theta).\left\{0.02552.\left[ln\left(\frac{E^*}{\sigma_{r\theta}}\right)\right]^3 - 0.72526.\left[ln\left(\frac{E^*}{\sigma_{r\theta}}\right)\right]^2 + 6.34493.\left[ln\left(\frac{E^*}{\sigma_{r\theta}}\right)\right] - 6.47458\right\}$$

→ the characteristic stress $\sigma_{r,\theta}$ per indenter

α-Al matrix characterization by nanoindentations

Indentations on grids with 3 different indenters → lowest curves for matrix

→ Swift or Voce hardening law fitting

infinity of solutions if σ_y not defined

→ σ_y from macro tensile test or analytical formula

→ Ok high ratio Si / α-Al strength & low fraction of Si particles

(Tran et al. 2022, under revision in Int. J. of Mech. Sc.)

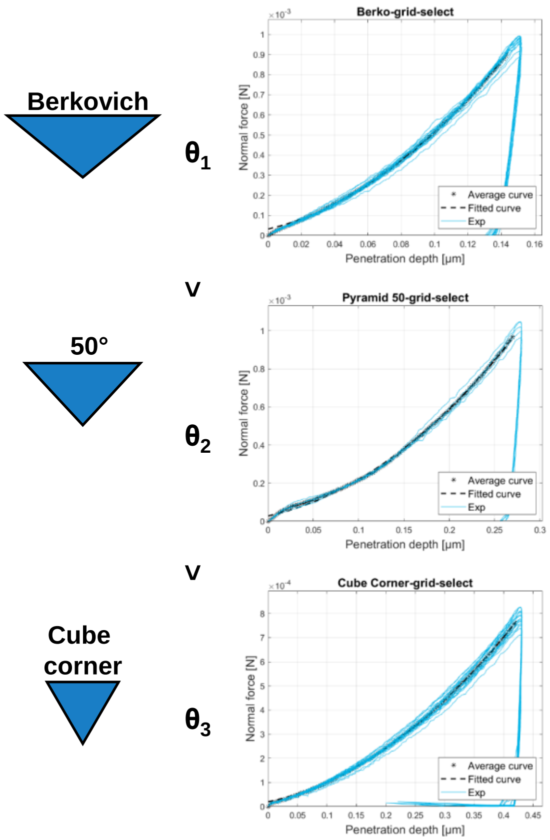

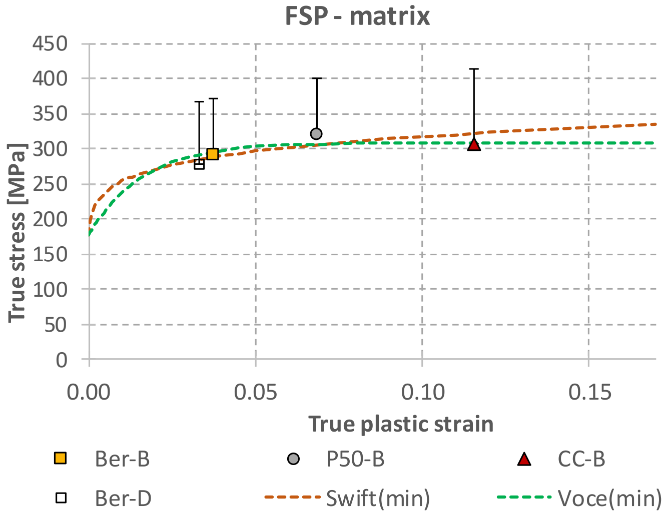

Data set B

≈ Data set A

(Dedry et al., ESAFORM PoPuPs, 2021)

Matrix + Particles → RVE

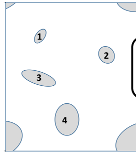

Small - 5 Si part.

Medium A – 10 Si part. & ≠ mesh sizes

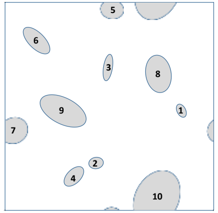

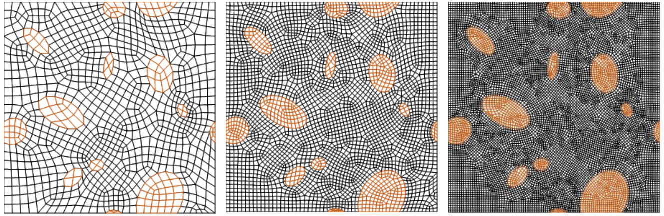

Medium B – 10 Si part.

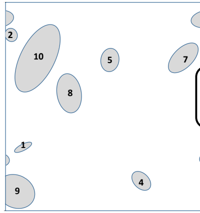

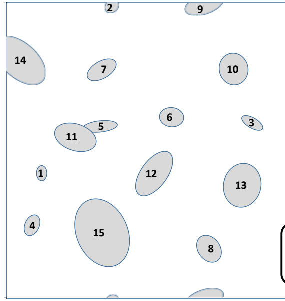

Large – 15 Si part.

Target: macro tensile test in Y dir.

≠ model, mesh sizes, 1 layer of 3D elements, 3D law

Macro level : $\varepsilon_{XX} \approx \varepsilon_{ZZ}$ (isotropic material)

Local level: strength in Z direction ≈ for all particles

(Bouffioux et al., 2022, nearly submitted)

Boundary conditions

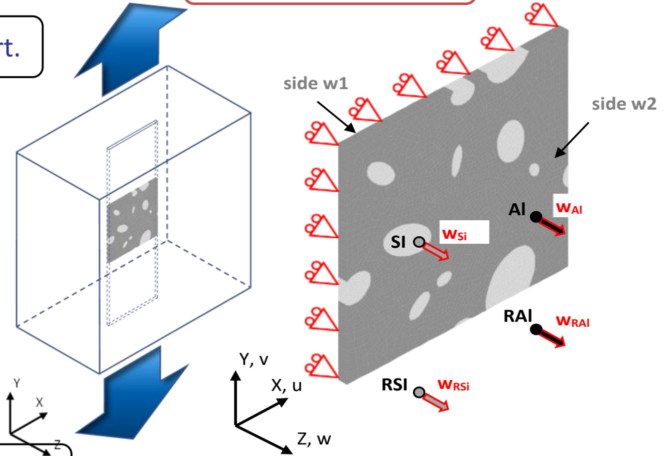

Strong strength ratio
Si particle / α-Al matrix

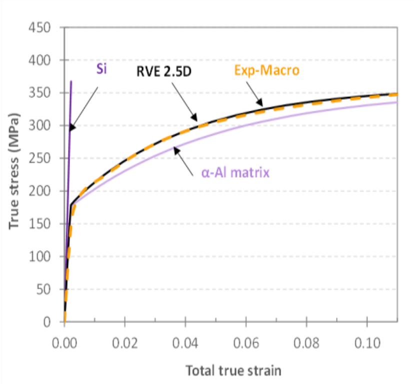

2D or 3D	→	**2.5D**
Representative Size	→	**10 particles**
Mesh density	→	**Fine**

Macroscopic σ - ε computed from RVE

Tensile test in y direction

Experimental validation

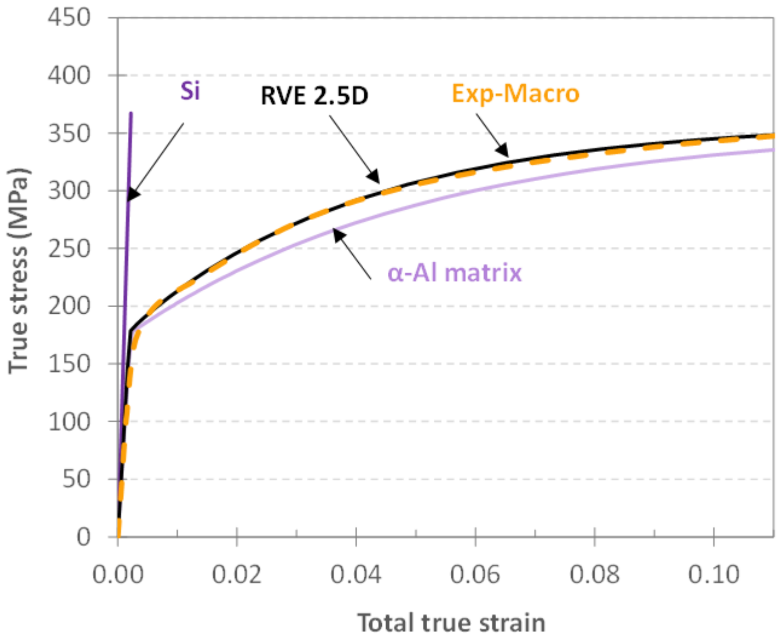

Effect of boundary conditions in Z direction

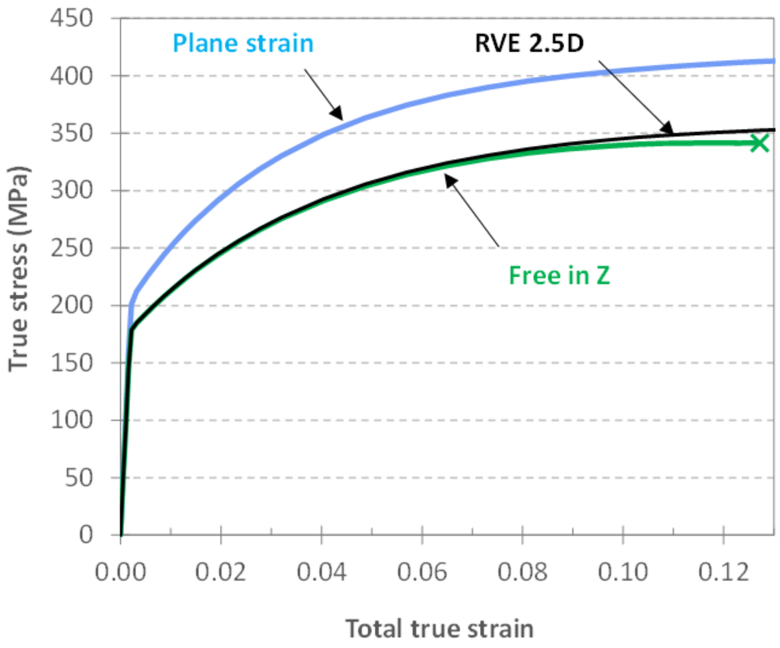

Sensitivity of local max σ_{yy} mesh & RVE size

Medium-A model
Macro deformation of 10%
σ_{YY} distribution [Mpa]

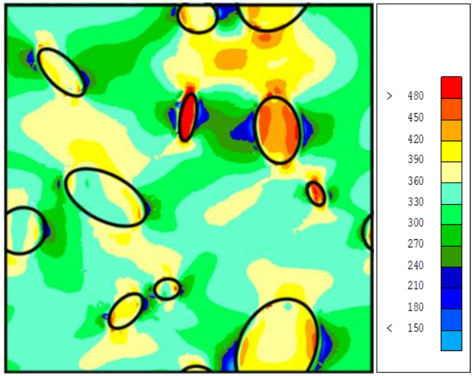

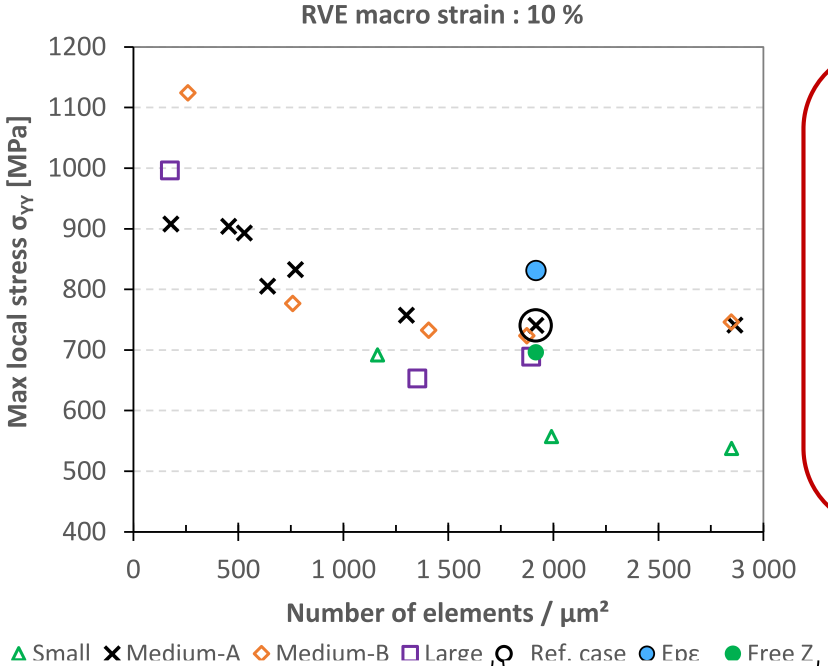

5 particles-mesh

→ not representative RVE

10 or 15 particles-meshes,

different Si part. distributions,

→ identical results

→ representative RVE

2.5D

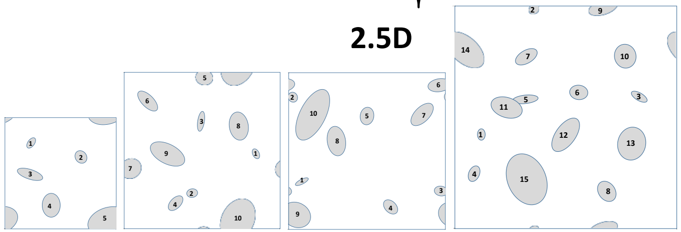

Effect of boundary conditions on medium-A RVE

→ Plane strain: too stiff

→ Free z : no stress in Z direction

Local stress field

RVE 2.5D
Periodic conditions in XY plane, force applied in Y

Effect of boundary conditions applied in Z direction

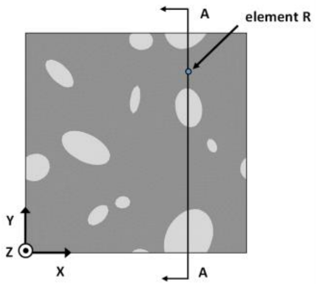

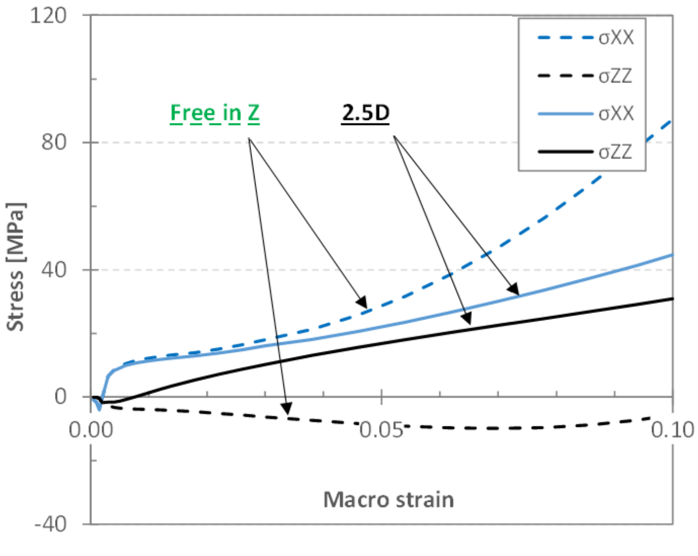

Stress distribution in Y & X directions

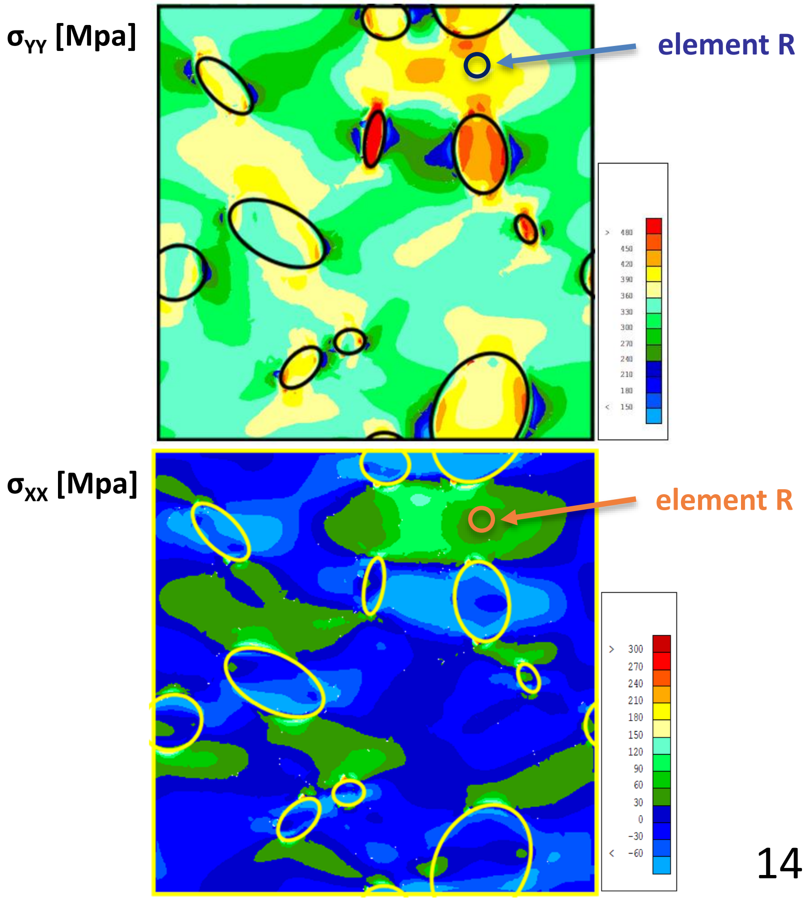

Damage mechanism in static loading → Cohesive interface elements

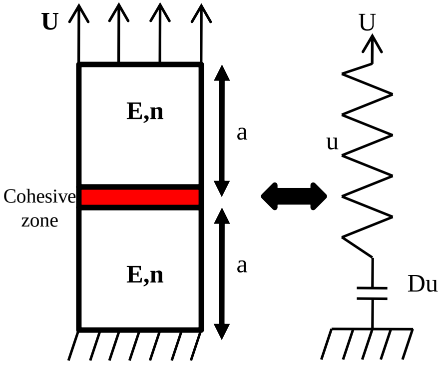

Uniaxial problem to illustrate the jump displacement

$$T = \begin{cases} \dfrac{\sigma_{max}}{\delta_0}\Delta u & \text{if } \Delta u < \delta_0 \\ \sigma_{max}\dfrac{\delta_c - \Delta u}{\delta_c - \delta_0} & \text{if } \delta_0 \le \Delta u \le \delta_c \\ 0 & \text{if } \Delta u > \delta_c \end{cases}$$

Bilinear law

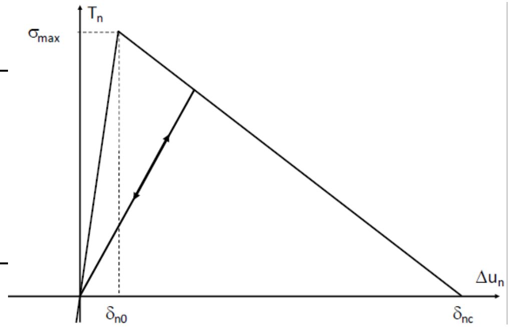

Traction separation law

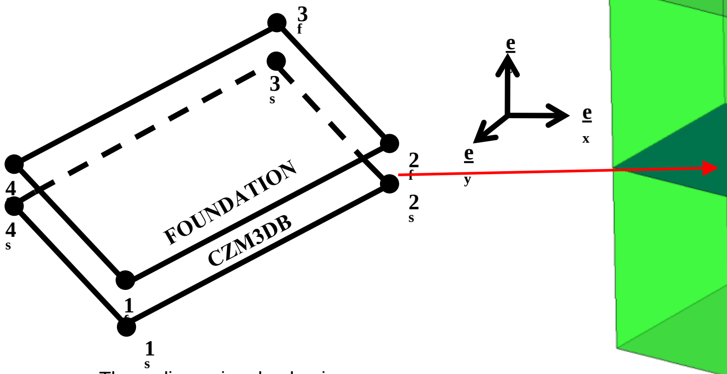

Three-dimensional cohesive zone

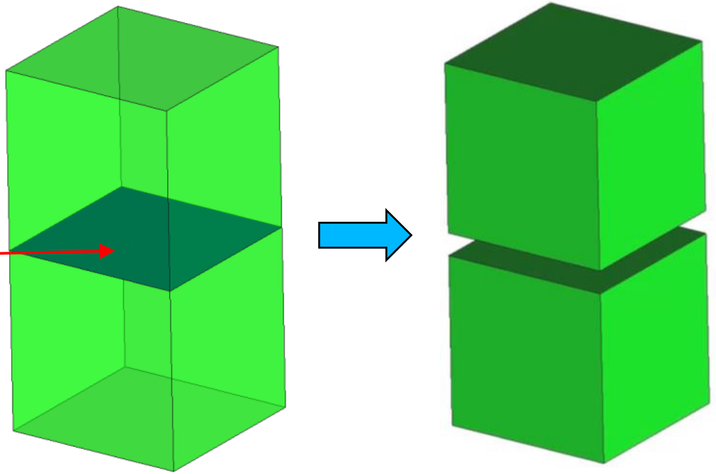

Cohesive zone modelling

Microstructure of AlSi10Mg after FSP

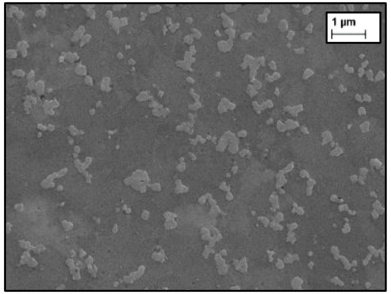

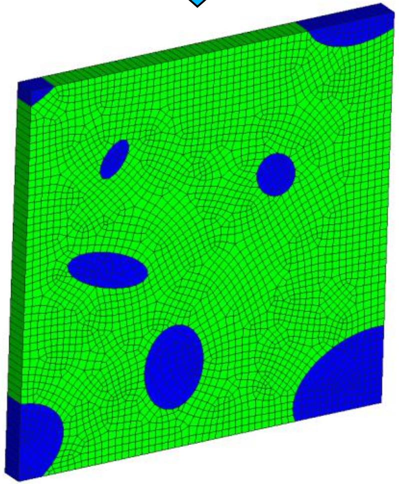

Finite element model of the Representative Volume Element (RVE)

σ_{max}	δ_{n0}	δ_{nc}	τ_{max}	δ_{t0}	δ_{tc}
550	5.5E-6	6E-6	550.	5.5E-6	6E-6

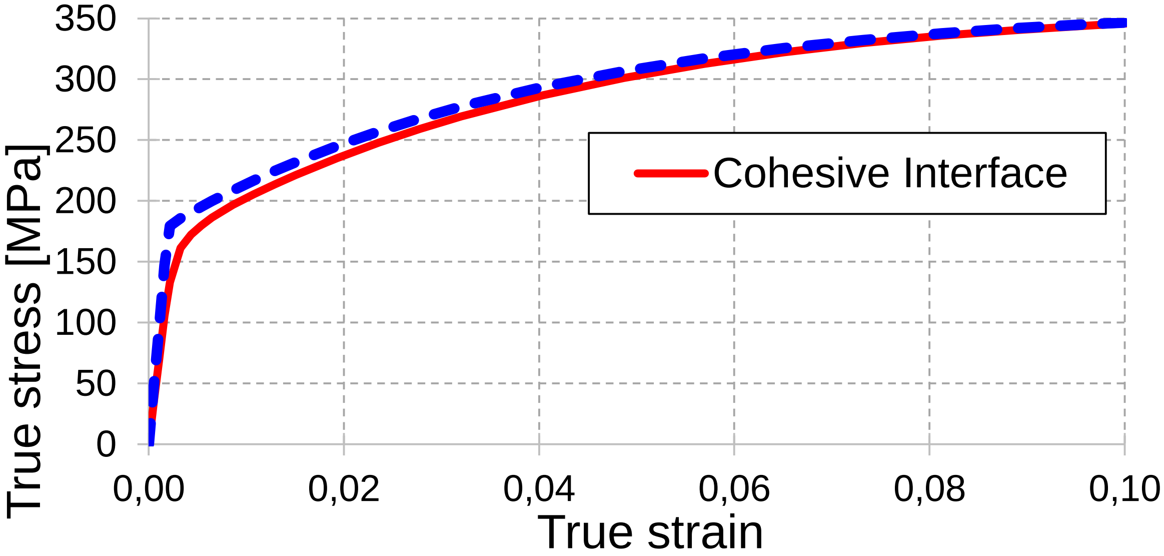

Sensitivity of local field assumption at macro strain 0.1

Perfect Interfaces

Cohesive Interfaces

Equivalent Strain

Tensile stress in Y direction

Stress-YY

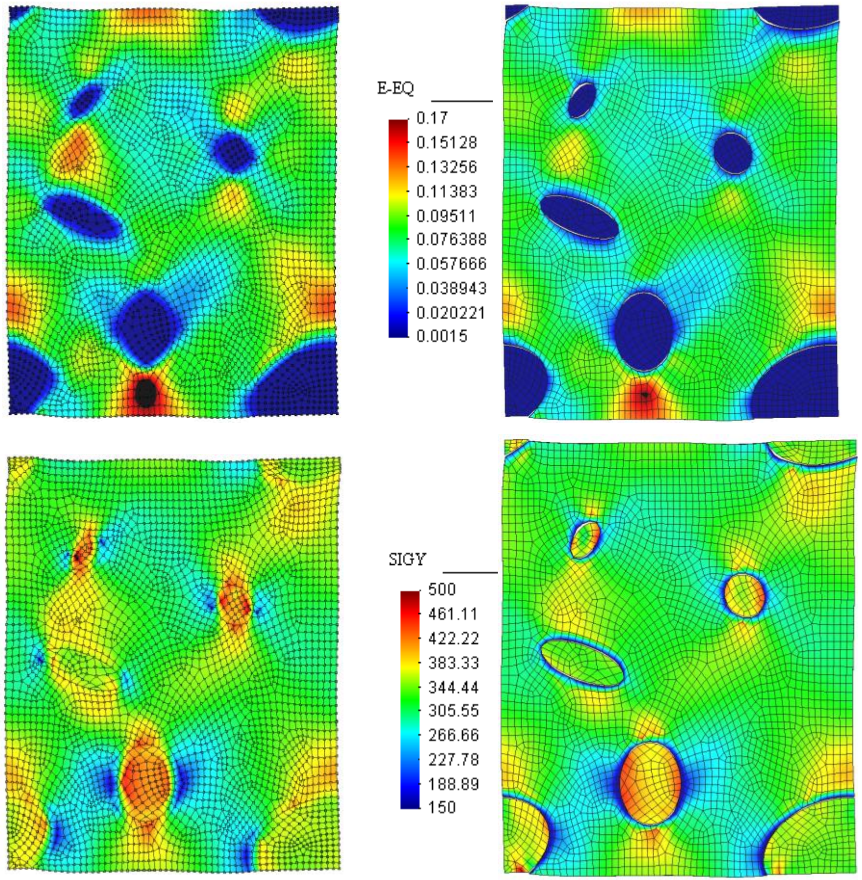

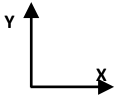

Decohesion starts at similar macro strain as experiment

RVE 2.5D ready to model fatigue

Conclusions Toward numerically optimized microstructure by RVE ?

Development of 2.5D RVE model → macro stress strain tensile curve validated
→ local stress and strain fields available
→ damage mechanism in static loading ongoing

A tool available for “isotropic matrix + precipitate material”

Input data from experiments here
However, Phase Field approach possible (see EMMC18 conf.)

Next steps: fatigue
→ Fatigue experimental campaign
→ RVE predictions via damage constitutive laws

LIÈGE université
Urban & Environmental Engineering

Thank you
Any questions ?

Anne.Habraken@uliege.be
Chantal.Bouffioux@uliege.be